Contribution from the Departments of Chemistry, Guelph-Waterloo Centre for Graduate Work in Chemistry, Guelph Campus, University of Guelph, Guelph, Ontario, Canada N1G 2W1, and Loyola University of Chicago, Chicago, Illinois 60626

Crystal Structure of 1,6-Biferrocenyl-2,5-dicyanohexa-1,3,5-triene and Intervalence Transfer in the Mixed-Valence Ion Based on This Structure

SULTAN I. AMER,[1a] GARFIELD SADLER,[1a] PATRICK M. HENRY,*[1a] GEORGE FERGUSON,*[1b] and BARBARA L. RUHL[1b]

Received May 30, 1984

Crystals of 1,6-biferrocenyl-2,5-dicyanohexa-1,3,5-triene are monoclinic, space group $P2_1/c$, with 2 molecules in a unit cell of dimensions a = 8.102 (1) Å, b = 10.595 (3) Å, c = 12.939 (4) Å, β = 95.14 (2)°, and R = 0.037 for 1594 reflections with $I > 3\sigma(I)$ measured by the diffractometer. The molecule is centrosymmetric with the nitrile group cis to the nearest ferrocene ring. In the ferrocene moiety the Fe–C distances are in the range 2.035–2.058 (3) Å; the two rings are 1.1 (4)° from being parallel and 3.8 (4)° from being eclipsed. The cyclic voltammogram in CH_3CN showed two overlapping waves for the oxidation of the two ferrocene centers. The potential difference, $\Delta E_{1/2}$ = 78 mV, corresponds to a constant, $K_c \cong 21$. The mixed-valence ion was generated electrochemically in a series of solvents. The ion displayed a low-energy band assigned to an intervalence electron-transfer (IT) transition between the two centers, and the energy of the band, E_{op}, showed the linear dependence on the dielectric properties of the solvent predicted by the Hush theory for weakly coupled systems. For the four ions Fc—Fc$^+$, Fc—C≡C—Fc$^+$, Fc—(C≡C)$_2$—Fc$^+$, and Fc—CH=C(CN)CH=CHC(CN)=CH—Fc$^+$ (Fc = ferrocenyl) the expected linear dependence between E_{op} and $1/d$ (d is the Fe–Fe distance) was also observed. These results as well as the IT band half-width, $\Delta\tilde{\nu}_{1/2}$, and α^2 indicate that the ion has essentially trapped valence with a slight degree of delocalization.

Introduction

Recent interest in mixed-valence complexes began after Creutz and Taube[2] reported, in 1969, the properties of the first discrete pyrazine-bridged ruthenium complex known as the Creutz–Taube ion. Cowan and co-workers followed by reporting the synthesis and properties of the monocation of biferrocene in 1970.[3] This work was extended to the first bridged biferrocene, Fc—C≡C—Fc, in 1974[4] and studies on Fc—C≡C—C≡C—Fc were reported in 1975.[5] Meyer et al.[6] have studied some bridged biferrocene ions where the internuclear separation between the metal centers has been extended.

The monocations of biferrocene[3] and bridged biferrocenes[4-6] were found to belong to class II in Robin and Day[7] classification and behave according to predictions by theories advanced by Hush[8] and Marcus[9] for weakly coupled systems.

We report here the crystal structure of 1,6-biferrocenyl-2,5-dicyanohexa-1,3,5-triene (I; Fc—CH=C(CN)CH=CHC(CN)=CH—Fc) and results of a study on the properties of the near-IR band in terms of solvent and internuclear distance dependence and extent of electron coupling between the redox centers. To our knowledge, this is the first biferrocenyl mixed-valence ion with a conjugated olefinic bridge.

Experimental Section

Materials. Tetra-*n*-butylammonium hexafluorophosphate (TBAH) was prepared according to a literature procedure.[10] Ferrocenecarboxaldehyde (Strem Chemicals) and 1,4-dicyanobut-2-ene (Aldrich Chemicals) were analytical reagent grade and were used as received. Acetonitrile (Burdick and Jackson Spectrograde) was dried over freshly activated alumina. All other solvents were of reagent grade and were dried over molecular sieves. Argon gas was purified as previously described.[11]

The compound Fc—CH=C(CN)CH=CHC(CN)=CH—Fc (I)[12] was prepared by the procedure of Sonogashira and Hagihara.[14] A saturated petroleum ether (30–60 M) solution was left in refrigerator (5 °C) for several days. Deep purple crystals suitable for X-ray structure determination were collected by filtration.

Table I. Atomic Coordinates for Non-Hydrogen Atoms (with Estimated Standard Deviations in Parentheses)

atom	x	y	z
Fe	0.17922 (4)	0.18775 (3)	0.11498 (3)
N	0.6875 (4)	0.2007 (3)	0.3412 (2)
C(11)	0.3378 (3)	0.0485 (3)	0.1682 (2)
C(12)	0.4256 (3)	0.1469 (3)	0.1205 (2)
C(13)	0.3598 (4)	0.1564 (3)	0.0163 (2)
C(14)	0.2316 (4)	0.0667 (3)	−0.0022 (2)
C(15)	0.2164 (4)	0.0006 (3)	0.0904 (2)
C(16)	0.3489 (3)	0.0045 (3)	0.2739 (2)
C(17)	0.4565 (3)	0.0371 (2)	0.3548 (2)
C(18)	0.4500 (3)	−0.0164 (2)	0.4582 (2)
C(19)	0.5832 (3)	0.1290 (3)	0.3440 (2)
C(21)	0.0639 (5)	0.2566 (4)	0.2375 (3)
C(22)	0.1560 (5)	0.3521 (4)	0.1954 (3)
C(23)	0.1013 (6)	0.3694 (3)	0.0933 (3)
C(24)	−0.0305 (5)	0.2856 (4)	0.0682 (3)
C(25)	−0.0546 (4)	0.2150 (4)	0.1567 (4)

Crystal Structure Analysis. Crystal Data: $C_{28}H_{22}Fe_2N_2$, M_r = 498.2, monoclinic, a = 8.102 (1) Å, b = 10.595 (3) Å c = 12.939 (4) Å, β = 95.14 (2)°, Z = 2, D_{calcd} = 1.50 g cm^{-3}, $F(000)$ = 512; Mo radiation, λ = 0.7107 Å, μ(Mo Kα) = 13.6 cm^{-1}; space group $P2_1/c$ uniquely from systematic absences $h0l$ ($l = 2n + 1$), $0k0$ ($k = 2n + 1$).

Accurate cell parameters were obtained by a least-squares refinement of the setting angles of 25 reflections (with θ between 10 and 15°) measured on an Enraf-Nonius CAD4 automatic diffractometer. Intensity data were collected with a small (0.11 × 0.41 × 0.54 mm) crystal to a maximum θ of 25°, and 1950 unique data were obtained. After corrections for Lorentz and polarization effects the data with $I > 3\sigma(I)$ (1594) were labeled observed and used in structure solution and refinement.

With Z = 2 the molecule must lie on a crystallographic inversion center. The coordinates of the unique Fe atom were obtained from an analysis of a three-dimensional Patterson function, and the remaining non-hydrogen atoms were located in a heavy-atom-phased Fourier summation. Refinement was by block-diagonal least-squares calculations[15] initially with isotropic and then with anisotropic vibration parameters. A difference map computed at an intermediate stage in the refinement revealed maxima in positions expected for all hydrogen atoms; these were then allowed for in geometrically idealized positions (C–H = 1.08 Å) and included, but not refined, in the final rounds of calculations. In the final

(1) (a) Loyola University of Chicago. (b) University of Guelph.
(2) Creutz, C.; Taube, H. *J. Am. Chem. Soc.* **1969**, *91*, 3988.
(3) Cowan, D. O.; Kaufman, F. *J. Am. Chem. Soc.* **1970**, *92*, 219.
(4) LeVande, C.; Cowan, D. O.; Leitch, C.; Bechgaard, K. *J. Am. Chem. Soc.* **1974**, *96*, 6788.
(5) LeVande, C.; Bechgaard, K.; Cowan, D. O. *J. Org. Chem.* **1976**, *41*, 2700.
(6) Power, M. J.; Meyer, T. J. *J. Am. Chem. Soc.* **1978**, *100*, 4393.
(7) Robin, M. B.; Day, P. *Adv. Inorg. Chem. Radiochem.* **1967**, *10*, 247.
(8) Hush, N. S. *Prog. Inorg. Chem.* **1967**, *8*, 391.
(9) Marcus, R. A. *Discuss. Faraday Soc.* **1960**, *29*, 11.
(10) Ferguson, J. A. Ph.D. Thesis, The University of North Carolina at Chapel Hill, 1971.
(11) Amer, S. I.; Dasgupta, T. P.; Henry, P. M. *Inorg. Chem.* **1983**, *22*, 1970.
(12) ($C_5H_5FeC_5H_4$)—CH=C(CN)CH=CHC(CN)=CH—($C_5H_4FeC_5H_5$). Anal. ($C_{28}H_{22}N_2Fe_2$) C, H, N.[13]
(13) Elemental Analysis was carried out by Guelph Chemical Laboratories, Guelph, Ontario, Canada.
(14) Sonogashira, K.; Hagihara, N. *Kogyo Kagaku Zasshi* **1963**, *66*, 1090.
(15) Larsen, A. C.; Gabe, E. J., "Computing in Crystallography"; Shenk, H., et al., Eds.; Delft University Press: Delft, 1978; pp 81–89.

0020-1669/85/1324-1517$01.50/0 © 1985 American Chemical Society

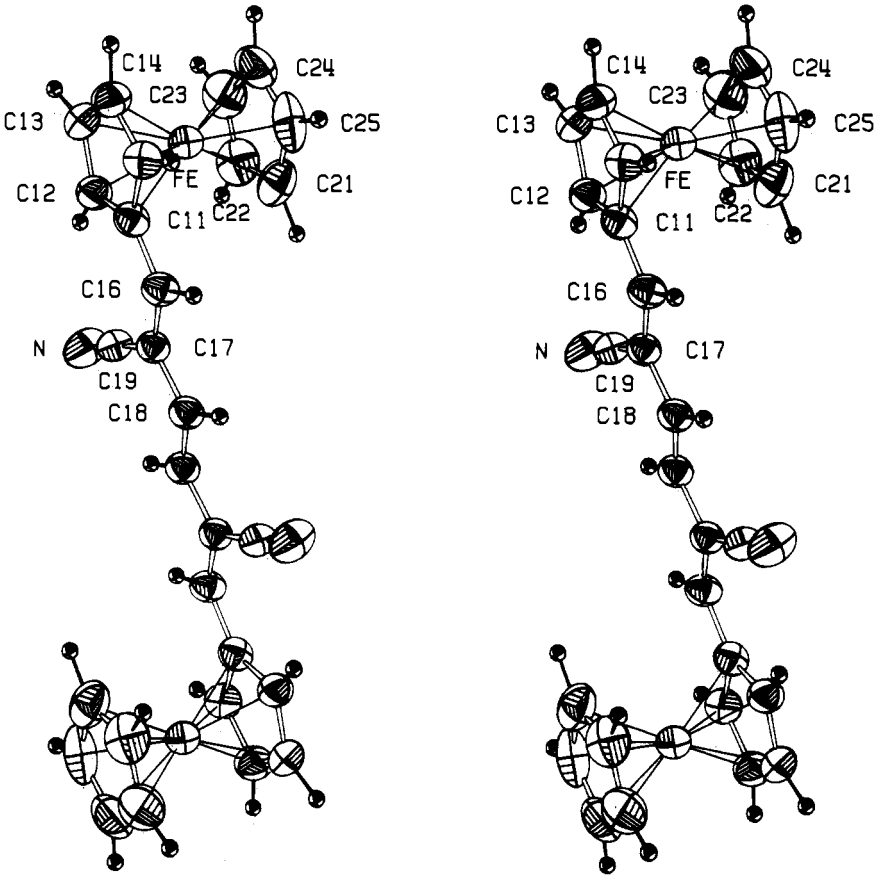

Figure 1. Stereoview of a molecule of I with our numbering scheme.

cycles of refinement a weighting scheme of the form $w = 1/\sigma^2(F)$ was employed. Scattering factors used in the structure factor calculations were taken from the literature,[16,17] and anomalous dispersion[18] was allowed for.

Refinement converged at $R = 0.0371$ and $R_w = 0.0534$ for the 1594 reflections with $I > 3\sigma(I)$. All shift/esd ratios in the last cycle were zero, and a final difference map contained no significant peaks. Coordinates of non-hydrogen atoms are given in Table I, and molecular dimensions are in Table II. Figure 1 shows a stereoview of the molecule with our numbering scheme, and Figure 2 is a stereoview of the unit cell contents. Figure 2 and listings of structure factors, calculated hydrogen coordinates, and anisotropic thermal parameters have been deposited as supplementary material.

Electrochemistry. Electrochemical measurements were conducted with a Bioanalytical Systems CV-1A voltammetry central unit or an IBM-EC/225 voltammetric analyzer combined with a three-electrode configuration. The mixed-valence ion was generated in solution by controlled-potential coulometry. Samples for spectral investigation were withdrawn by syringe technique to a 1-cm quartz cell equipped with an air-tight Teflon cap. Spectral measurements were run as quickly as possible (10–15 min) due to the instability of the ion.

Reduction potentials for the Fc^+–Fc^0 couples in a series of solvents (containing 0.1 M TBAH) were measured vs. the saturated calomel electrode (SCE). Cyclic voltammograms showed two[19] unresolved waves resulting from the stepwise oxidation of the two Fe centers. Values of $E_{1/2}(1)$ and $E_{1/2}(2)$ were estimated by using the method outlined by Richardson and Taube.[21] The values of $\Delta E_{1/2}$, as measured against the SCE, showed dependence on solvent properties.

Table II. Molecular Dimensions (with Estimated Standard Deviations in Parentheses)

(a) Bond Lengths (A)

Fe-C(11)	2.037 (3)	C(11)-C(16)	1.440 (4)
Fe-C(12)	2.038 (3)	C(12)-C(13)	1.409 (4)
Fe-C(13)	2.052 (3)	C(13)-C(14)	1.413 (5)
Fe-C(14)	2.058 (3)	C(14)-C(15)	1.402 (4)
Fe-C(15)	2.035 (3)	C(16)-C(17)	1.348 (4)
Fe-C(21)	2.044 (3)	C(17)-C(18)	1.459 (3)
Fe-C(22)	2.045 (4)	C(17)-C(19)	1.430 (4)
Fe-C(23)	2.038 (4)	C(18)-C(18)' [a]	1.339 (5)
Fe-C(24)	2.036 (4)	C(21)-C(22)	1.396 (6)
Fe-C(25)	2.035 (3)	C(21)-C(25)	1.426 (6)
N-C(19)	1.139 (4)	C(22)-C(23)	1.368 (6)
C(11)-C(12)	1.432 (4)	C(23)-C(24)	1.405 (7)
C(11)-C(15)	1.438 (4)	C(24)-C(25)	1.396 (7)

(b) Bond Angles (deg)

C(12)-C(11)-C(15)	106.8 (2)	C(16)-C(17)-C(19)	121.3 (2)
C(12)-C(11)-C(16)	130.8 (2)	C(18)-C(17)-C(19)	116.0 (2)
C(15)-C(11)-C(16)	122.2 (2)	C(17)-C(18)-C(18)' [a]	124.8 (2)
C(11)-C(12)-C(13)	107.7 (3)	C(17)-C(19)-N	176.1 (3)
C(12)-C(13)-C(14)	108.9 (3)	C(22)-C(21)-C(25)	106.7 (4)
C(13)-C(14)-C(15)	108.1 (3)	C(21)-C(22)-C(23)	109.6 (4)
C(14)-C(15)-C(11)	108.5 (3)	C(22)-C(23)-C(24)	108.3 (4)
C(11)-C(16)-C(17)	129.6 (2)	C(23)-C(24)-C(25)	107.9 (4)
C(16)-C(17)-C(18)	122.7 (2)	C(24)-C(25)-C(21)	107.6 (3)

[a] The primed atom is obtained from the coordinates of Table I by the operation $1-x, -y, 1-z$.

The potential difference, $\Delta E_{1/2} = E_{1/2}(2) - E_{1/2}(1) = 78$ mV in CH_3CN, corresponds to a comproportionation constant, K_c, of 21 for the equilibrium in eq 1. With the value for K_c of 21 the equilibrium mixture,

$$[Fc^+ \rightsquigarrow Fc^+] + [Fc^0 \rightsquigarrow Fc^0] \overset{K_c}{\rightleftharpoons} 2[Fc^+ \rightsquigarrow Fc^0] \qquad (1)$$

after coulometry, was found to be ≃70% in the mixed-valence ion. As $\Delta E_{1/2}$ changed slightly in other solvents, so did the corresponding K_c and the percentage of the monocation in the equilibrium mixture. Oxidation

(16) Cromer, D. T.; Mann, J. B. *Acta Crystallogr., Sect. A: Cryst. Phys., Diffr. Theor. Gen. Crystallogr.* **1968**, *A24*, 321.
(17) Stewart, R. F.; Davidson, E. R.; Simpson, W. T. *J. Chem. Phys.* **1965**, *42*, 3175.
(18) Cromer, D. T.; Liberman, D. *J. Chem. Phys.* **1970**, *53*, 1891.
(19) That compound I undergoes two one-electron processes and not a two-electron process is demonstrated by the large difference in oxidative and reductive peak potentials (>150 mV). For a two-electron process a difference of 30 mV should be expected.[20]
(20) Nicholson, R. S.; Shain, I. *Anal. Chem.* **1964**, *36*, 706.
(21) Richardson, D. E.; Taube, H. *Inorg. Chem.* **1981**, *20*, 1278.

Table III. Half-Wave Potentials[a] for I in Various Solvents[b]

	cyclic voltammetry			differential pulse				
solvent	$E_p - E_{p/2}$/mV	$E_{1/2}(1)$, $E_{1/2}(2)$/mV	$\Delta E_{1/2}$/mV	width/mV	$E_{1/2}(1)$, $E_{1/2}(2)$/mV	$\Delta E_{1/2}$/mV	K_c	%(3,2)
acetone	106	618, 534	84	155	618, 540	78	21	70
acetonitrile	102	573, 493	80	156	578, 500	78	21	70
benzonitrile	97	650, 574	76	144	643, 572	71	16	67
butyronitrile	106	647, 563	84	150	646, 571	75	19	68
methylene chloride	97	708, 632	76	141	712, 642	70	15	66

[a] Using a Pt-foil working electrode. [b] Containing 0.1 M TBAH.

Table V. Data for Intervalence-Transfer Bands of I in Different Solvents[a]

				$\Delta\bar{\nu}_{1/2}/\mu m^{-1}$		X_o/cal mol^{-1}	
solvent	$1/D_{op} - 1/D_s$	$\bar{\nu}_{max}/\mu m^{-1}$	ϵ_{max}[b]/M^{-1} cm^{-1}	obsd	calcd	obsd	calcd
acetone	0.493	0.899	267	0.457	0.456	19.9	26.7
acetonitrile	0.526	0.966	120	0.517	0.472	21.1	28.4
benzonitrile	0.388	0.765	275	*c*	0.420	15.6	21.0
butyronitrile	0.473	0.873	213	0.572	0.449	19.0	25.6
propylene carbonate	0.481	0.889	102	0.485	0.453	19.4	26.0

[a] At 25 °C; containing 0.1 M TBAH. [b] Corrected for K_c. [c] Unsymmetrical narrow band.

by one electron produced the mixed-valence ion, and solutions were used for spectral measurements. Data are shown in Table III.

Spectral Data. Ultraviolet–visible and near-infrared spectra were obtained on Cary 14 or Perkin-Elmer 330 spectrophotometers. The infrared spectrum was recorded using a Perkin-Elmer 180 spectrophotometer.

Ultraviolet–Visible Spectrum. The spectrum of I in ethanol, as reported by Hagihara and co-worker,[14] displayed two bands in range of 800–300 nm (ϵ_{520} = 8300, ϵ_{380} = 38700). The present work shows that the spectrum has other features that were not previously reported. Thus, as shown in Figure 3, the high-energy band is certainly unsymmetrical and can be resolved into a band at 382 nm and a shoulder at 363 nm, with the molar extinction coefficients for both the 526 nm (ϵ = 4432) (present work) and 382 nm (ϵ = 17340) bands being about half the literature values. Furthermore, two other transitions were observed below 350 nm: a shoulder at 305 nm and a band at 272 nm (ϵ = 34370). In agreement with the work of Lundquist and Cais[22] and by comparison with ferrocene, Hagihara et al.[14] assigned the 526- and 382-nm bands to transitions between the metal and the cyclopentadienyl rings. Furthermore, they concluded that each Fe ring unit absorbs independently. Recently, Morrison and Hendrickson[23] assigned the high-energy band(s) in ferrocene to ligand-to-metal charge-transfer transitions and the low-energy one to a transition arising from excitation of an electron from an MO that is mainly metal to one that is ligand in character (MLCT). This assignment can be extended to the ferrocene part of I; the 526-nm band is an MLCT or ligand field transition while the 382- and 363-nm bands are assigned to LMCT transitions.[24] The nitrile group influenced the positions of the two major bands compared with the non-nitrile bearing analogue (see compounds VIIIa and X in Table I in ref 11). The red shift observed when the nitrile groups were introduced was greater for the long-wavelength band compared with that for the short-wavelength band (66 nm vs. 16 nm). The two transitions below 350 nm are assigned to $\pi \rightarrow \pi^*$ transitions in the hexatriene bridge.

Infrared Spectrum. The spectrum was measured as a KBr pellet and shown to be rich in bands in the range 3500–300 cm^{-1}. The bands and their assignments are shown in Table IV, which has been deposited as supplementary material. All characteristic ferrocene bands[25] are displayed: ν(C–H) in the range 3140–3025 cm^{-1}; ring ν(C–C) between 1403 and 1348 cm^{-1}; δ(C–H) from 1251 to 1000 cm^{-1} as weak bands. Ring distortion is in the ranges 903–840 and 651–620 cm^{-1}. Ring–metal–ring stretches appear between 518 and 480 cm^{-1}, ring tilt appears between 420 and 402 cm^{-1}, and ν(ring–metal) appears at 312 cm^{-1}.

Vibrations for the 2,5-dicyanohexa-1,3,5-triene part are also displayed; most of the common modes are in the same ranges as those for the ferrocene part. The whole molecule is centrosymmetric, and accordingly the central ν(C=C) was not expected to appear in the infrared spectrum. The other ν(C=C) appeared as a very sharp band at 1593 cm^{-1}. The ν(C≡N) showed up as a sharp band at 2219 cm^{-1}. Out-of-plane δ(C–H) deformation is at 811 cm^{-1} and P(C—C≡N) between 518 and 500 cm^{-1}. Other frequencies and their assignment are shown in Table IV.

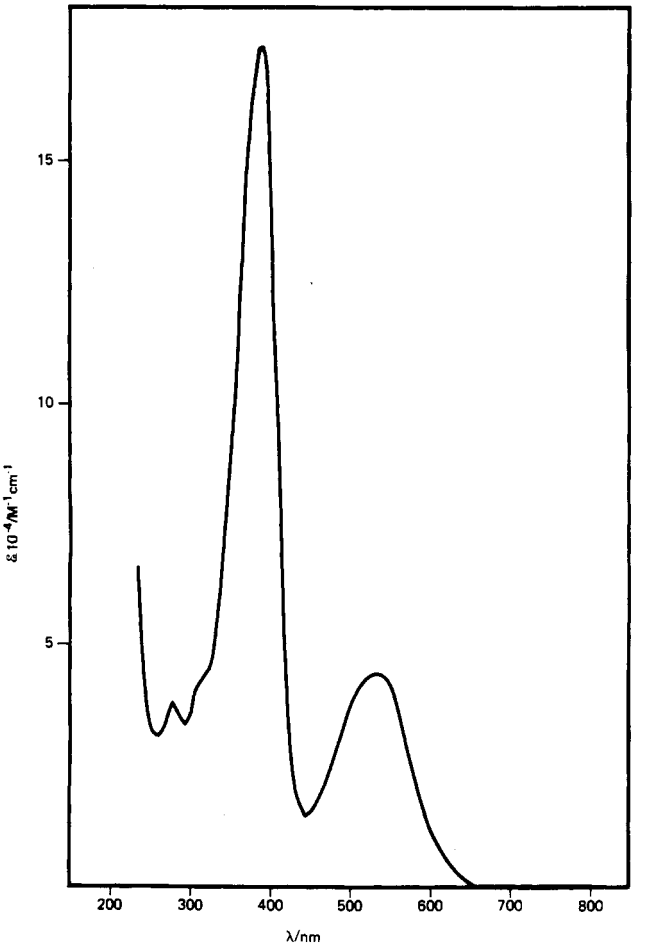

Figure 3. Spectrum of I in ethanol.

Intervalence-Transfer Band. The mixed-valence ion of I displayed a well-defined band in the near-infrared region that is assignable to a light-induced electron transfer[7,8] from the ferrocene to the ferrocenium moiety. This band is absent in both the neutral molecule and doubly oxidized ion. The energy of this band, E_{op}, showed the expected solvent dependence.[8] Variations of E_{op} as a function of the dielectric properties

(22) Lundquist, R. T.; Cais, M. *J. Org. Chem.* **1962**, *27*, 1167.
(23) Morrison, W. H.; Hendrickson, D. N. *Inorg. Chem.* **1975**, *14*, 2331.
(24) A reviewer has suggested that the 526-nm band more likely arises from ligand field transitions since a similar absorption in ferrocene is generally given this assignment.
(25) Hyams, I. *J. Spectrochim. Acta, Part A* **1973**, *29A*, 839. Many of the bands have several components.

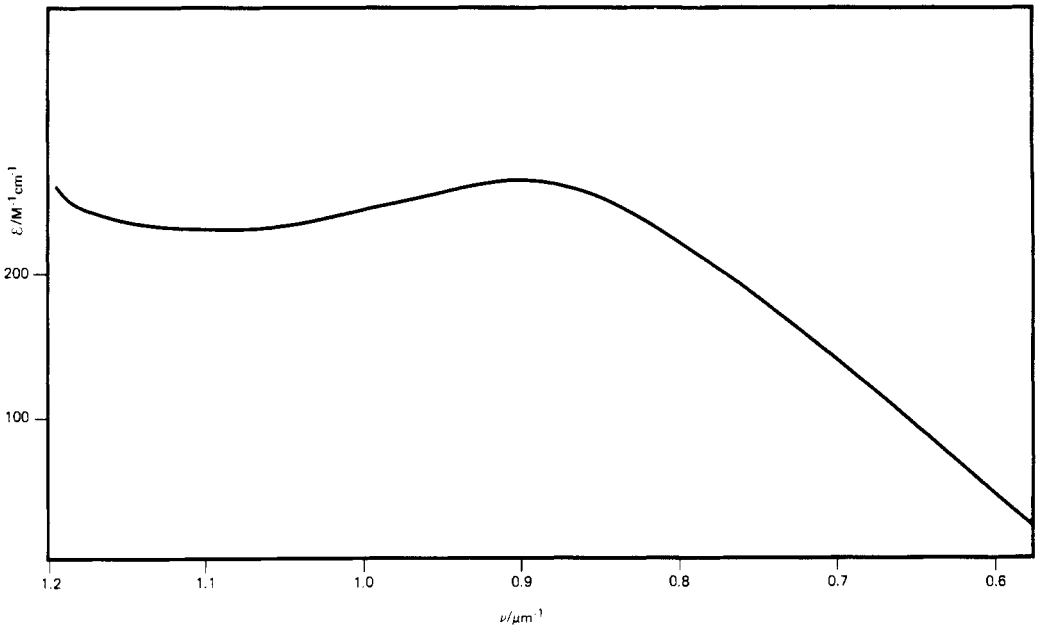

Figure 4. Intervalence-transfer band for I^+ in acetone.

of a series of solvents[26] as well as other properties are listed in Table V. Figure 4 shows the IT band in acetone; the band appears essentially Gaussian[8] in shape. A plot of E_{op} vs. $(1/(D_{op} - 1/D_s)$, where D_{op} and D_s are the optical and static dielectric constants for the solvent, is shown in Figure 5. The straight line has an intercept of 0.213 μm^{-1}, a slope of 141 μm^{-1}, and a correlation coefficient, r^2, of 0.986.

Discussion

X-ray Structure. The crystal structure of I contains discrete, well-resolved centrosymmetric molecules, with only van der Waals contacts between them. In the molecule, shown in Figure 1, the cyclopentadienyl rings are 1.1 (4)° from being parallel and 3.8 (4)° from being eclipsed. The rings are each planar to within 0.005 Å. The iron atom is 1.650 (3) and 1.657 (3) Å from each plane. In the ferrocene moiety, mean dimensions are Fe–C = 2.042 (3)°, C–C = 1.411 (5) Å, and C–C–C = 108.0 (3)°. These dimensions are in accord with those for ferrocene[27] (mean C–C = 1.415 (4) Å, mean Fe–C = 2.039 (3) Å) and its derivatives[28] (mean C–C = 1.420 (10) Å, mean Fe–C = 2.046 (9) Å). The unsubstituted ring, not unexpectedly, shows substantially greater thermal motion than the substituted one that is bonded to the polyolefinic chain. The $C_5H_4C{=}C(CN)C{=}CC(CN){=}CC_5H_4$ chain is maximally extended, with a maximum deviation from planarity of 0.09 Å. The bond lengths in the chain (mean $C_{sp^2}{=}C_{sp^2}$ = 1.344 (4) Å, mean $C_{sp^2} - C_{sp^2}$ = 1.450 (4) Å) shows a clear differentiation between double and single bonds with little delocalization between them. The above values are in accord with those found in other ferrocene derivatives, e.g. in (2,2-dicyanovinyl)ferrocene[28] (mean C–C = 1.448 (5) Å, C=C = 1.375 (5) Å).

In the centrosymmetric molecule, the Fe···Fe separation required in calculations outlined below is 11.535 (1) Å. The cis configuration of the C_5H_4 ring and the CN group about the C(16)=C(17) double bond results in some overcrowding that is relieved by (a) bond angle bending [e.g., C(12)–C(11)–C(16) is increased to 130.8 (2)° (cf. C(15)–C(11)–C(16) = 122.2 (2)°), C(11)–C(16)–C(17) is increased to 129.6 (2)° (cf. C(17)–C(18)–C(18′) = 124.8 (2)°), and C(17)–C(19)–N is changed to 176.1 (3)° from linear (away

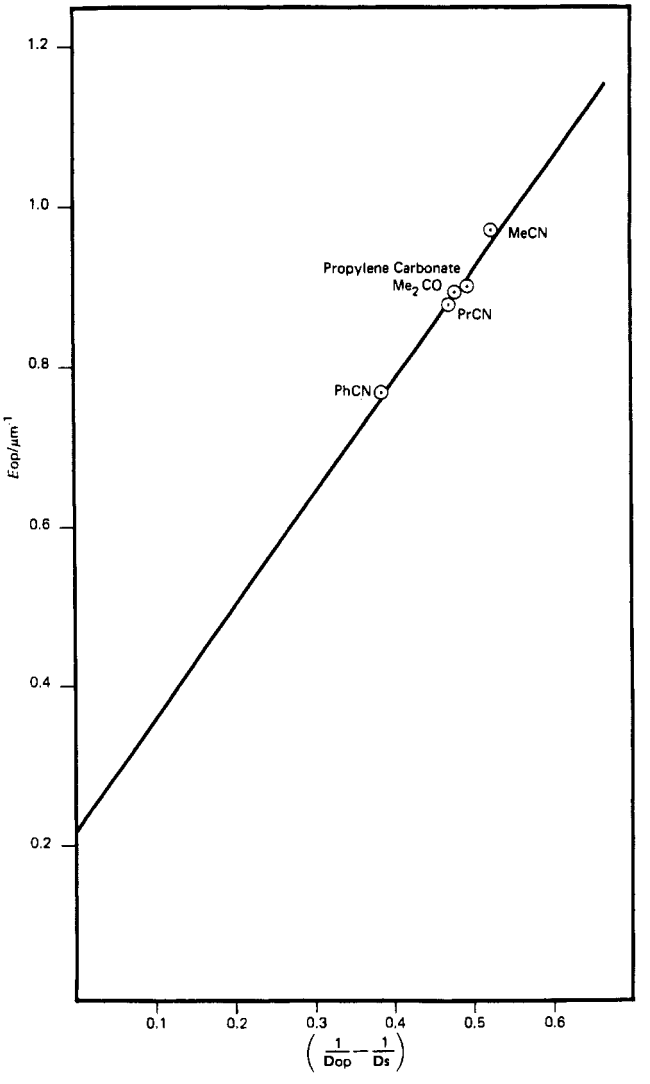

Figure 5. Plot of E_{op} vs. $(1/D_{op} - 1/D_s)$ for I^+ in various solvents.

(26) Solvents such as dimethyl sulfoxide, dimethylformamide, propionitrile, and tetrahydrofuran were excluded[6] since the cyclic voltrammogram appeared ill shaped (only an oxidative peak appeared). In methylene chloride, we obtained a reasonable CV but no IT bands were observed.

(27) (a) Takusagawa, F.; Koetz, T. F. *Acta Crystallogr., Sect. B: Struct. Crystallogr. Cryst. Chem.* **1979**, *B35*, 1074. (b) Sieler, P.; Dunitz, J. D. *Acta Crystallogr., Sect. B: Struct. Crystallogr. Cryst. Chem.* **1979**, *B35*, 2020.

(28) (a) Krukonis, A. P.; Silverman, J.; Yannoni, N. F. *Acta Crystallogr., Sect. B: Struct. Crystallogr. Cryst. Chem.* **1972**, *B28*, 987. (b) Einstein, F. W. B.; Willis, A. C. *Acta Crystallogr., Sect. B: Struct. Crystallogr. Cryst. Chem.* **1980**, *B36*, 39. (c) Gromek, J. M.; Donohue, J. *Cryst. Struct. Commun.* **1981**, *10*, 597. (d) Skrzypczak-Jankin, E.; Hoser, A.; A.; Grzesiak, E.; Kaluski, Z. *Acta Crystallogr., Sect. B: Struct. Crystallogr. Cryst. Chem.* **1980**, *B36*, 934.

from C(12))] and (b) rotation about the exocyclic C(11)–C(16) bond (torsion angle C(12)–C(11)–C(16)–C(17) = −6.8 (4)°).

Electrochemistry. The results in Table III clearly indicate that the mixed-valence ion of I has the properties predicted[7] for weakly interacting or valence-trapped systems. The potential difference, $\Delta E_{1/2}$, measured in a series of solvents corresponds to a low value for the comproportionation equilibrium constant, K_c (15–21), that, although slightly above the statistical value of 4, indicates that interaction between the Fe(II) and Fe(III) sites is quite weak. The value of $\Delta E_{1/2}$, in a given solvent, was reported[4] for mixed-valence ions of biferrocene and other biferrocenes bridged by π-unsaturated groups and shown to decrease as the internuclear separation between the metal sites increased.[29] The larger value ($\Delta E_{1/2}$ = 0.350 V) for biferrocene is not in line with those observed for bridged biferrocenes.[5] As discussed by Taube,[30] $\Delta E_{1/2}$ on depends on the properties of all three species (Fc–Fc, Fc^+–Fc^+, Fc–Fc^+) in the equilibrium mixture and may not be a direct measure of electronic delocalization between the sites.

Intervalence-Transfer Transition. Evidence that the mixed-valence ion of I belongs to class II is provided by the appearance of a new band in the near-IR region similar to those observed for other biferrocenes[5] and polyferrocenes[31] and pentaammineruthenium mixed-valence compounds (see for example ref 11 and references therein). The band is absent in both the neutral compound and doubly oxidized ion. The band in acetone is shown in Figure 4. In CH_3CN the band appeared at 1035 nm with an extinction coefficient, ϵ_{max}, of 120 M^{-1} cm^{-1} and was essentially Gaussian.[8] The appearance of the band is attributed to an intervalence electron-transfer transition between the donor and acceptor sites leaving the ion in a vibrationally excited state:

$$[Fe^{II}\text{–}Fe^{III}] \xrightarrow{h\nu} [Fe^{III}\text{–}Fe^{II}]^* \qquad (2)$$

This intervalent transfer (IT) transition is an indication and measure of the extent of electronic coupling between the two centers, which are separated by the long triene ligand (r = 11.53 Å obtained from our X-ray structural determination).

The band width at half-height, $\Delta\tilde{\nu}_{1/2}$, is related to its energy by a simple relationship of the form

$$\Delta\tilde{\nu}_{1/2} = 48.06(\tilde{\nu}_{IT})^{1/2} \qquad (3)$$

where $\Delta\tilde{\nu}_{1/2}$ and $\tilde{\nu}_{IT}$ are in cm^{-1}. Values for $\Delta\tilde{\nu}_{1/2}$ measured in different solvents are listed in Table V.

Solvent Dependence. The plot, shown in Figure 5, shows the linear relationship between E_{op} and $1/D_{op} - 1/D_s$), where D_{op} and D_s are the optical and static dielectric constants of the solvent. For weakly coupled cases, Hush[8] showed that E_{op} can be given in terms of the inner-sphere X_i (involving metal–ligand bond length changes following the act of electron transfer) and outer-sphere X_o (involving solvent reorganization between reactant and product). The two terms are well separated in energy and are additive parts of the total X in eq 4. In the high-temperature limit, $\hbar\omega$

$$E_{op} = X = X_i + X_o \qquad (4)$$

$\ll kT$, and if dielectric saturation and specific solute solvent interaction can be ignored, the outer-sphere term, X_o, can be treated by the dielectric continuum theory advanced by Marcus[32] and Hush[8] according to eq 5 where N is Avogadro's number, e

$$X_o = \frac{Ne^2}{4\pi\epsilon_0}\left(\frac{1}{2a_1} + \frac{1}{2a_2} - \frac{1}{r}\right)\left(\frac{1}{D_{op}} + \frac{1}{D_s}\right) \qquad (5)$$

is the electronic charge, ϵ_0 is the permeability in vacuum, a_1 and a_2 are the molecular radii of the donor and acceptor sites, and r is the internuclear distance between them. D_{op} and D_s are previously defined. The straight line in Figure 5 has an intercept X_i of 0.213 μm^{-1} and a slope of 1.41 μm^{-1}. Using equation 5 and values for $a_1 \equiv a_2$ = 4.0 Å and r = 11.5 Å the calculated slope has a value of 1.89 μm^{-1}. The discrepancy between the calculated and experimental values for the slope arises from the inherent approximate nature of the dielectric continuum model used in the calculation and the fact that the calculation is quite sensitive to the chosen values for a_1, a_2, and r; if a value of $a_1 = a_2$ = 4.4 Å were chosen, both experimental and calculated slopes would be the same. Accordingly, X_o in CH_3CN evaluated from the slope of the line in Figure 5 has a value of 21.2 kcal mol^{-1}, in fair agreement with the calculated value 28.4 kcal mol^{-1}.

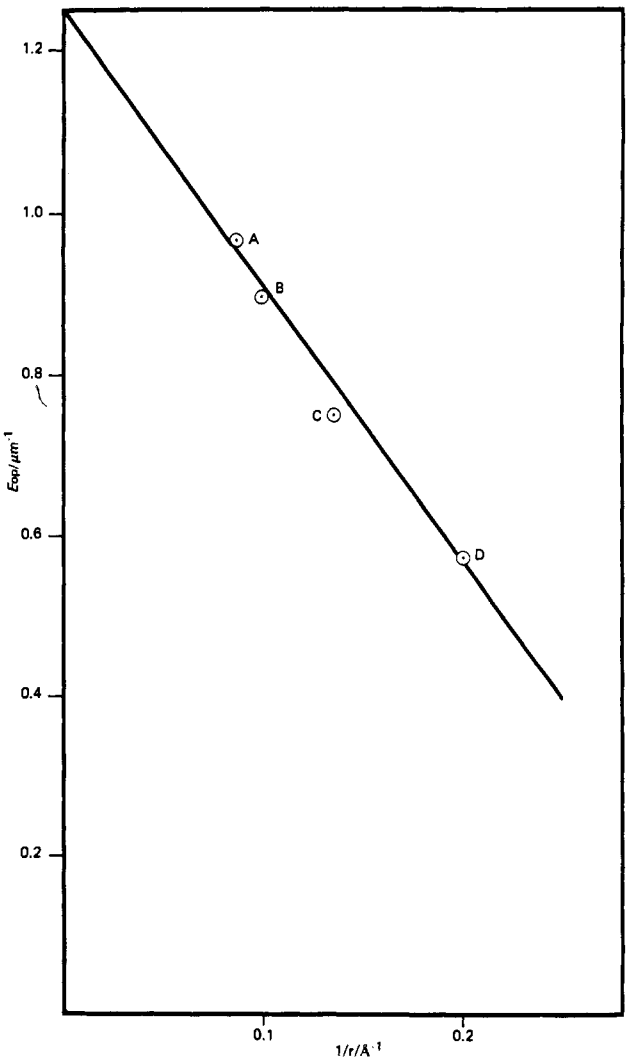

Figure 6. Plot of E_{op} vs. $1/r$ for a series of four biferrocene ions: (A) Fc—CH=C(CN)CH=CHC(CN)=CH—Fc^+; (B) Fc—$(C\equiv C)_2$—Fc^+; (C) Fc—C≡C—Fc^+; (D) Fc—Fc^+.

Distance Dependence. Equations 4 and 5 show that the E_{op} of the IT transition is a function of internuclear separation, r, between the interacting centers. If the equation is rearranged to give eq 6, a linear dependence of E_{op} on $1/r$ is obtained. The distance

$$E_{op} = X = X_i + \frac{Ne^2}{4\pi\epsilon_0}\left(\frac{1}{a}\right)\left(\frac{1}{D_{op}} - \frac{1}{D_s}\right) - \frac{Ne^2}{4\pi\epsilon_0}\left(\frac{1}{r}\right)\left(\frac{1}{D_{op}} - \frac{1}{D_s}\right) \qquad (6)$$

dependence occurs only in the outer-sphere reorganizational term since both the donor and acceptor sites should behave as uncoupled oscillators as required by Hush's theory[8] for weakly interacting systems. In Figure 6 is shown a plot of E_{op} in CH_3CN–0.1 M TBAH vs. $1/r$ for a series of four closely related biferrocene ions that have identical molecular radii (a = 4.0 Å; Fc—Fc^+, Fc—C≡C–Fc^+, Fc—$(C\equiv C)_2$—Fc^+,[33] Fc—CH=C(CN)CH=CHC-

(29) Except for biferrocene ($E_{1/2}$ = 0.350 V) a linear relationship between $E_{1/2}$ and r was found.
(30) Taube, H. *Ann. N.Y. Acad. Sci.* **1978**, *313*, 485.
(31) Brown, G. M.; Meyer, T. J.; Cowan, D. O.; LeVanda, C.; Kaufman, F.; Roling, P. V.; Rausch, M. D. *Inorg. Chem.* **1975**, *14*, 506.
(32) (a) Marcus, R. A. *J. Chem. Phys.* **1955**, *24*, 966. (b) Marcus, R. A. *Ann. Rev. Phys. Chem.* **1964**, *15*, 155.

Table VI. Slopes and X_i's from Plots of E_{op} vs. $1/D_{op} - 1/D_s$ for a Series of Biferrocene Mixed-Valence Ions

ion	E_{op}[a]/μm^{-1}	$X_i/\mu m^{-1}$	slope/μm^{-1} calcd	slope/μm^{-1} obsd	ν/Å
Fc–Fc$^+$ [b]	0.568	0.353	0.654	0.412	5.00
Fc–C≡C–Fc$^+$ [b]	0.747	0.281	1.19	0.908	7.30
Fc–(C≡C)$_2$–Fc$^+$ [c]	0.895	0.247[d]			9.97
Fc–CH=C(CN)CH=CHC(CN)=CH–Fc$^+$	0.966	0.213	1.89	1.41	11.5

[a] In CH_3CN–0.1 M TBAH. [b] Values are taken from ref 5. [c] See ref 30. [d] Assumed since solvent dependence was not carried out for this ion.

(CN)=CH—Fc$^+$). The calculated value for the intercept (with an average X_i = 0.274 μm^{-1} for the four ions; see Table VI) is 1.84 μm^{-1} compared to the experimental value of 1.25 μm^{-1}. The experimental slope of the line in Figure 6 is −3.45 μm^{-1} compared to the calculated one of −6.09 μm^{-1}. The experimental slope of the line in Figure 6 is −3.45 μm^{-1} compared to the calculation one of −6.09 μm^{-1}. That the experimental value of the slope is smaller than calculated is due to the fact that the derivation of eq 6 requires that $r \geq (a_1 + a_2)$ (the distance of closest approach), which holds true only for Fc—(C≡C)$_2$—Fc and Fc—CH=C-(CN)CH=CHC(CN)=CH—Fc. If the line were drawn through these two points, the appropriate slope is obtained, −5.89 μm^{-1} (≅3.3% smaller than that calculated). Other sources for the discrepancy[34] between experimental and calculated values for both slope and intercept are, again, due to the oversimplified nature of the dielectric continuum model.

Delocalization in the Mixed-Valence Ion of I. Properties of mixed-valence ions depend upon the extent of electronic interaction, α, in the ground state between the two sites. The definition of α is given in eq 7, ϕ_i and ϕ_j are wave functions for the donor

$$\psi_G = (1 - \alpha^2)^{1/2}\phi_i + \alpha\phi_j \quad (7)$$

and acceptor sites in the mixed-valence state. The intensity (oscillator strength $f = 2.9 \times 10^{-3}$) of the IT transition depends upon the transition dipole moment, μ, between the ground, ψ_G, and excited, ψ_E, states where G and E are mixed donor, ϕ_i, and acceptor, ϕ_j, wave function (eq 8). From first-order perturbation

$$\mu = \langle\psi_G|er|\psi_E\rangle \quad (8)$$

theory[36] the transition dipole moment is given by eq 9, where e

$$\mu = \alpha er = 7.99 \times 10^{-11}\ \text{e Å} \quad (9)$$

is the electronic charge. Consequently, the intensity depends upon the square of both the internuclear distance, r, and the interaction parameter, α, where α^2 can be calculated by eq 10. A value of

$$\alpha^2 = \frac{(4.2 \times 10^{-4})\epsilon_{max}\Delta\tilde{\nu}_{1/2}}{E_{op}r^2} \quad (10)$$

$\alpha^2 = 2 \times 10^{-4}$ for the ion satisfies the requirement for trapped valence, $\alpha < 0.25$.[36] Other parameters for the IT transition such as the length of the dipole moment (D = 0.166 Å) and the mixing parameter ($a = 1.44 \times 10^{-2}$) support the conclusion that the ion has essentially trapped valence.[37]

The theory of Hush[8] predicts that for the symmetrical case the optical energy E_{op} of the IT transition is equal to the Frank–Condon barrier to electron transfer, E_{FC}. In addition to the optical path, a thermally activated process occurs during formation of the transition state and the two processes are related by

$$E_{th} = \frac{E_{op}}{4} - \beta = \frac{E_{FC}}{4} - \beta \quad (11)$$

where β is the resonance interaction energy between ϕ_i and ϕ_j wave functions and its value for the ion in hand is 0.017 V. The calculated E_{th} = 6.51 kcal mol^{-1} yields a first-order rate constant for electron transfer, $k_{et} = 2 \times 10^8\ s^{-1}$.

Conclusion. The structure of the neutral compound 1,6-biferrocenyl-2,5-dicyanohexa-1,3,5-triene shows the molecule to be centrosymmetric, with a fully extended almost planar C_5H_4C=C(CN)C=CC(CN)=CC_5H_4 moiety and with very little delocalization in the hexatriene chain. The mixed-valence ion of I belongs to class II as evidenced by the value of K_c and from properties of the IT band that indicated that although the two sites are separated by r = 11.5 Å they still interact through the conjugated bridge.

Acknowledgment. The support of the Natural Sciences and Engineering Research Council of Canada (to P.M.H. and G. F.) is gratefully acknowledged. S.I.A. was a visiting Professor in the Chemistry Department of Loyola University during the 1982–1983 academic year.

Registry No. I, 1273-49-0; Fe—CH=C(CN)CH=CHC(CN)=CH—Fc$^+$, 95406-93-2.

Supplementary Material Available: Listings of infrared data (Table IV), hydrogen coordinates, thermal parameters, mean plane data, and observed and calculated structure amplitudes and Figure 2, a stereoview of the unit cell contents (20 pages). Ordering information is given on any current masthead page.

(33) Cowan et al.[4] reported a value for E_{op} = 0.847 μm^{-1} for the ion in CH_2Cl_2–0.1 M n-Bu_4NBF_4. After correction for both solvent and supporting electrolyte a value of 0.895 μm^{-1} was obtained and used to construct the plot in Figure 6.
(34) An empirical correction was developed by Meyer et al.[35] to correct for this kind of discrepancy and applied to a series of diruthenium dimers.
(35) Powers, M. J.; Meyer, T. J. *J. Am. Chem. Soc.* **1980**, *102*, 1289.
(36) Mayoh, B.; Day, P. *J. Am. Chem. Soc.* **1972**, *94*, 2885.
(37) For a definition of these terms see: Sutton, J. E.; Sutton, P. M.; Taube, H. *Inorg. Chem.* **1979**, *18*, 1017.